Journal of Nonlinear Modeling and Analysis https://global-sci.com/jnma
Volume 8, Number 2, April 2026, 305–322 DOI:10.12150/jnma.2026.305

Dynamical Analysis in a Discrete Fractional Order Harvested Predator-Prey Model Incorporating Fear Effect and Refuge

Siti Nurul Afiyah[1,2], Fatmawati[3,†] and Windarto[3]

Received 25 October 2024; Accepted 2 November 2025

Abstract This paper examines the dynamics of a discrete fractional-order predator-prey model, incorporating the effects of fear, prey refuge, and population harvesting. The fractional-order framework, which accounts for memory-dependent processes, provides a more accurate depiction of biological interactions than traditional integer-order models. Fear is modeled as a factor that reduces predator-prey encounters, while prey refuge offers a sanctuary, altering population dynamics. The inclusion of harvesting further complicates prey population regulation. We identify the system's equilibrium points and conduct a local stability analysis, focusing on the conditions that lead to stability, instability, and bifurcation. Specifically, we examine the Neimark-Sacker bifurcation, where a stable fixed point evolves into a closed periodic orbit. Numerical simulations corroborate the analytical findings, illustrating the pivotal roles that fear, refuge, and harvesting play in shaping system stability and long-term behavior.

Keywords Dynamical analysis, predator-prey model, harvesting, fear effect, refuge, discrete fractional order

MSC(2010) 37N30, 34A08.

1. Introduction

Mathematical models in ecology have become important tools for understanding complex dynamics in ecosystems. One of the most studied models is the predator-prey model, which is used to explore interactions between predator and prey populations [1]. One of the well-known predator and prey models is the Lotka-Volterra model introduced by Lotka (1925) and Volterra (1926). One intriguing aspect of the predator-prey model is its ability to produce periodic population patterns, where

†the corresponding author.
Email address:noeroel@asia.ac.id(S. N. Afiyah), fatmawati@fst.unair.ac.id(F. Fatmawati),windarto@fst.unair.ac.id(W. Windarto)
[1]Doctoral Program of Mathematics and Natural Science, Faculty of Science and Technology, Universitas Airlangga, Surabaya, Indonesia
[2]Department of Computer Science, Institut Teknologi dan Bisnis Asia, Malang 65113, Indonesia
[3]Department of Mathematics, Faculty of Science and Technology, Universitas Airlangga, Surabaya 60115, Indonesia

the numbers of predators and prey rise and fall in repeated cycles. Wild animals like wolves and gazelles or lions and zebras exhibit this [2].

Predator-prey models have been used widely in ecology to understand species interactions, develop conservation strategies, and predict the impacts of environmental change on animal populations. Furthermore, in the last few decades, many researchers have developed the predator-prey model by modifying the model by adding functional response [3, 4], refuge on prey [5–8] and/or refuge on predators [9], fear effects [10–13], cannibalism [15–17], harvesting [18–20], and various other modifications.

Moreover, from a mathematical perspective, the predator-prey model can be represented as a set of differential equations. The system of integer-order differential equations signifies that the rate of population expansion is influenced by factors beyond the current state. Nevertheless, it is an established truth that the rate of population change is influenced by all preceding conditions, a phenomenon referred to as the memory effect. The phenomenon of memory retention is referred to as fractional order. A system is considered memoryless if its output at any given time t is completely determined by the input at the same time t. A memory system, on the other hand, is used to retain the previous input value in order to calculate the current output value [21].

Fractional order differential equation systems have the ability to provide a real picture of biological phenomena compared to integer order. This fractional differential equation model provides a more accurate description than first-order dynamic systems for complex natural dynamics [22]. The development of fractional order predator-prey models has increased researchers' interest in analyzing fractional order dynamical systems [23–28]. Zhang et al. [29] examined the impact of adding fear effect and prey refuge in a Holling type II predator-prey model. Zhang et al. conducted a study on the influence of fear on the model and discovered that fear not only decreases the population density of the predator but also brings stability to the system. Harvesting is one of the additional factors that influence the dynamics of predator and prey populations. Harvesting of populations is a crucial factor in predator-prey dynamics, as highlighted by Sarkar et al. [30] in their study on the subject. Inspired by this study, we did research on a fractional-order harvesting predator-prey model that incorporates the fear effect and refuge for the prey. The model is as follows:

$$\begin{aligned} {}^{C}D^{\alpha}P(t) &= \frac{r_1 P}{1+fQ} - bP^2 - \frac{\nu(1-\delta)PQ}{1+\eta(1-\delta)P} - z_1(1-\delta)P, \\ {}^{C}D^{\alpha}Q(t) &= -r_2 Q + \frac{c\nu(1-\delta)PQ}{1+\eta(1-\delta)P} - z_2 Q, \end{aligned} \tag{1.1}$$

where condition $P(0) > 0, Q(0) > 0$. Here P and Q are the prey and predator populations, respectively, r_1 is the intrinsic growth of the prey, f is the level of fear, b is the intrinsic growth rate per carrying capacity of prey, c is the efficiency of food conversion from prey to predator, z_1 is the harvesting rate of the prey, r_2 is the predator natural death rate, η is the interaction coefficient, ν is the coefficient of predation, and z_2 is the harvesting rate of the predator.

The predator-prey model with a fractional order in continuous time can be expressed as a nonlinear differential equation. Finding the precise solution to the continuous fractional order predator-prey model is a challenging task. Hence, the utilization of a numerical method is necessary to facilitate the identification of an approach for solving fractional order differential equations that cannot be simply identified using analytical means [31]. The numerical approach that is often used in research is using the method used by Diethelm [32] which has been studied and used by Elsadany [33] and Panigoro [34]. This method is known as Piecewise Constant Arguments (PWCA). The Piecewise Constant Arguments (PWCA) approach has been widely used by several researchers in dynamic analysis [35–40]. These researchers revealed that discrete systems have richer dynamic behavior compared to continuous systems. Therefore, we are interested in conducting research on dynamic model (1.1) in discrete form. Based on the researcher's knowledge, the discrete form of model (1.1) has not been researched. In this research, in the discretization process, we used the Piecewise Constant Arguments (PWCA) method. This research examines the fractional predator-prey model, which takes into account the impact of fear, refuge on prey, and harvesting in both populations.

2. Dicretization process

In this section, we follow [34, 40] to process the discretization of system (1.1) using the piecewise constant arguments (PWCA) scheme. The PWCA of system (1.1) is as follows:

$$\begin{aligned}
{}^{C}D^{\alpha}P(\tau) =& \frac{r_1 P\left(\left[\frac{\tau}{h}\right]h\right)}{1+fQ\left(\left[\frac{\tau}{h}\right]h\right)} - b\left(P\left(\left[\frac{\tau}{h}\right]h\right)\right)^2 - \frac{\nu(1-\delta)P\left(\left[\frac{\tau}{h}\right]h\right)Q\left(\left[\frac{\tau}{h}\right]h\right)}{1+\eta(1-\delta)P\left(\left[\frac{\tau}{h}\right]h\right)} \\
& - z_1(1-\delta)P\left(\left[\frac{\tau}{h}\right]h\right), \\
{}^{C}D^{\alpha}Q(\tau) =& -r_2 Q\left(\left[\frac{\tau}{h}\right]h\right) + \frac{c\nu(1-\delta)P\left(\left[\frac{\tau}{h}\right]h\right)Q\left(\left[\frac{\tau}{h}\right]h\right)}{1+\eta(1-\delta)P\left(\left[\frac{\tau}{h}\right]h\right)} - z_2 Q\left(\left[\frac{\tau}{h}\right]h\right),
\end{aligned} \tag{2.1}$$

with initial state $P(0) = P_0$, $Q(0) = Q_0$ and the step size $h > 0$.

Let $\tau \in [0, h)$, $\frac{\tau}{h} \in [0, 1)$. According to equation (2.1), we have

$$\begin{aligned}
{}^{C}D^{\alpha}P(\tau) &= \frac{r_1 P_0}{1+fQ_0} - bP_0^2 - \frac{\nu(1-\delta)P_0 Q_0}{1+\eta(1-\delta)P_0} - z_1(1-\delta)P_0, \\
{}^{C}D^{\alpha}Q(\tau) &= -r_2 Q_0 + \frac{c\nu(1-\delta)P_0 Q_0}{1+\eta(1-\delta)P_0} - z_2 Q_0.
\end{aligned} \tag{2.2}$$

The solution to this fractional differential equation can be expressed as:

$$\begin{aligned}
P_1(\tau) &= P_0 + \frac{\tau^{\alpha} P_0}{\Gamma(1+\alpha)}\left[\frac{r_1}{1+fQ_0} - bP_0 - \frac{\nu(1-\delta)Q_0}{1+\eta(1-\delta)P_0} - z_1(1-\delta)\right], \\
Q_1(\tau) &= Q_0 + \frac{\tau^{\alpha} Q_0}{\Gamma(1+\alpha)}\left[-r_2 + \frac{c\nu(1-\delta)P_0}{1+\eta(1-\delta)P_0} - z_2\right].
\end{aligned} \tag{2.3}$$

Let $\tau \in [h, 2h)$, $\frac{\tau}{h} \in [1, 2)$. According to equation (2.1), we have

$$\begin{aligned}
{}^{C}D^{\alpha}P(\tau) &= \frac{r_1 P_1}{1+fQ_1} - bP_1^2 - \frac{\nu(1-\delta)P_1 Q_1}{1+\eta(1-\delta)P_1} - z_1(1-\delta)P_1, \\
{}^{C}D^{\alpha}Q(\tau) &= -r_2 Q_1 + \frac{c\nu(1-\delta)P_1 Q_1}{1+\eta(1-\delta)P_1} - z_2 Q_1.
\end{aligned} \tag{2.4}$$

The solution to this fractional differential equation can be expressed as:

$$\begin{aligned} P_2(\tau) &= P_1 + \frac{(\tau-h)^\alpha P_1}{\Gamma(1+\alpha)}\left[\frac{r_1}{1+fQ_1} - bP_1 - \frac{\nu(1-\delta)Q_1}{1+\eta(1-\delta)P_1} - z_1(1-\delta)\right], \\ Q_2(\tau) &= Q_1 + \frac{(\tau-h)^\alpha Q_1}{\Gamma(1+\alpha)}\left[-r_2 + \frac{c\nu(1-\delta)P_1}{1+\eta(1-\delta)P_1} - z_2\right]. \end{aligned} \tag{2.5}$$

Let $\tau \in [2h, 3h)$, $\frac{\tau}{h} \in [2,3)$. According to equation (2.1), we have

$$\begin{aligned} {}^C D^\alpha P(\tau) &= \frac{r_1 P_2}{1+fQ_2} - bP_2^2 - \frac{\nu(1-\delta)P_2Q_2}{1+\eta(1-\delta)P_2} - z_1(1-\delta)P_2, \\ {}^C D^\alpha Q(\tau) &= -r_2Q_2 + \frac{c\nu(1-\delta)P_2Q_2}{1+\eta(1-\delta)P_2} - z_2Q_2. \end{aligned} \tag{2.6}$$

The solution to this fractional differential equation can be expressed as:

$$\begin{aligned} P_3(\tau) &= P_2 + \frac{(\tau-h)^\alpha P_2}{\Gamma(1+\alpha)}\left[\frac{r_1}{1+fQ_2} - bP_2 - \frac{\nu(1-\delta)Q_2}{1+\eta(1-\delta)P_2} - z_1(1-\delta)\right], \\ Q_3(\tau) &= Q_2 + \frac{(\tau-h)^\alpha Q_2}{\Gamma(1+\alpha)}\left[-r_2 + \frac{c\nu(1-\delta)P_2}{1+\eta(1-\delta)P_2} - z_2\right]. \end{aligned} \tag{2.7}$$

Furthermore, By iterating the procedure n times, we obtain

$$\begin{aligned} {}^C D^\alpha P(\tau) &= \frac{r_1 P_n}{1+fQ_n} - bP_n^2 - \frac{\nu(1-\delta)P_nQ_n}{1+\eta(1-\delta)P_n} - z_1(1-\delta)P_n, \\ {}^C D^\alpha Q(\tau) &= -r_2Q_n + \frac{c\nu(1-\delta)P_nQ_n}{1+\eta(1-\delta)P_n} - z_2Q_n. \end{aligned} \tag{2.8}$$

For $\tau \in [nh, (n+1)h)$, $\frac{\tau}{h} \in [n, n+1)$. In accordance with the equation (2.1), we have solutions

$$\begin{aligned} P_{n+1}(\tau) &= P_n + \frac{(\tau-nh)^\alpha P_n}{\Gamma(1+\alpha)}\left[\frac{r_1}{1+fQ_n} - bP_n - \frac{\nu(1-\delta)Q_n}{1+\eta(1-\delta)P_n} - z_1(1-\delta)\right], \\ Q_{n+1}(\tau) &= Q_n + \frac{(\tau-nh)^\alpha Q_n}{\Gamma(1+\alpha)}\left[-r_2 + \frac{c\nu(1-\delta)P_n}{1+\eta(1-\delta)P_n} - z_2\right]. \end{aligned} \tag{2.9}$$

Next, taking $\tau \to (n+1)h$, equation (2.9) yields

$$\begin{aligned} P_{n+1} &= P_n + \frac{h^\alpha P_n}{\Gamma(1+\alpha)}\left[\frac{r_1}{1+fQ_n} - bP_n - \frac{\nu(1-\delta)Q_n}{1+\eta(1-\delta)P_n} - z_1(1-\delta)\right], \\ Q_{n+1} &= Q_n + \frac{h^\alpha Q_n}{\Gamma(1+\alpha)}\left[-r_2 + \frac{c\nu(1-\delta)P_n}{1+\eta(1-\delta)P_n} - z_2\right]. \end{aligned} \tag{2.10}$$

3. Equilibrium points and local stability of equilibrium points

This section focuses on the existence of equilibrium points and their local stability. In order to examine the presence of equilibrium points and their local stability, it is necessary to utilize the lemma provided below:

Lemma 3.1. *[34] Consider a difference equation*

$$x_{n+1} = f(x_n), x \in \Re^2. \tag{3.1}$$

An equilibrium point of equation (3.1) is defined as a point $x^* \in \Re^2$ that fulfills the equation $x^* = f(x^*)$. Let $\lambda_i, i = 1, 2$ represent the eigenvalues of the Jacobian matrix at the equilibrium point x^* of equation (3.1). The equilibrium point x^* is determined as follows:

1. *locally asymptotically stable (sink) if $|\lambda_1| < 1$ and $|\lambda_2| < 1$; or*
2. *unstable (source) if $|\lambda_1| > 1$ and $|\lambda_2| > 1$; or*
3. *unstable (saddle) if $|\lambda_1| > 1$ and $|\lambda_2| < 1$; or $|\lambda_1| < 1$ and $|\lambda_2| > 1$; or*
4. *non-hyperbolic if $|\lambda_1| = 1$ and $|\lambda_2| = 1$.*

Lemma 3.2. *[34] Let the characteristic equation of Jacobian matrix at equilibrium point $F(\lambda) = \lambda^2 - Tr\lambda + Det$. Suppose that $F(1) > 0$, and $\lambda_i, i = 1, 2$ are roots of $F(\lambda) = 0$. Then*

1. *$|\lambda_1| < 1$ and $|\lambda_2| < 1$ if and only if $F(-1) > 0$ and $Det < 1$.*
2. *$|\lambda_1| > 1$ and $|\lambda_2| > 1$ if and only if $F(-1) > 0$ and $Det > 1$.*
3. *$|\lambda_1| > 1$ and $|\lambda_2| < 1$, or $|\lambda_1| < 1$ and $|\lambda_2| > 1$ if and only if $F(-1) < 0$.*
4. *$\lambda_1 = -1$ and $\lambda_2 \neq 1$ if and only if $F(-1) = 0$ and $Tr \neq 0, 2$, and*
5. *λ_1 and λ_2 are complex and $|\lambda_1| = |\lambda_1| = 1$ if and only if $Tr^2 - 4Det < 0$ and $Det = 1$.*

To determine the presence of the equilibrium point of system (2.10), we solve the following equation:

$$\begin{aligned} P &= P + \frac{h^\alpha P}{\Gamma(1+\alpha)}\left[\frac{r_1}{1+fQ} - bP - \frac{\nu(1-\delta)Q}{1+\eta(1-\delta)P} - z_1(1-\delta)\right], \\ Q &= Q + \frac{h^\alpha Q}{\Gamma(1+\alpha)}\left[-r_2 + \frac{c\nu(1-\delta)P}{1+\eta(1-\delta)P} - z_2\right]. \end{aligned} \tag{3.2}$$

We identify three equilibrium points, which are as follows:

1. The trivial equilibrium point $E_0 = (0, 0)$, which always exists.
2. The predator free equilibrium point $E_1 = (\frac{r_1 - z_1(1-\delta)}{b}, 0)$, which exists under the condition $r_1 > z_1(1-\delta)$.
3. The interior equilibrium point $E_2 = (P^*, Q^*)$, where $P^* = \frac{r_2+z_2}{(1-\delta)(c\nu - \eta(r_2+z_2))}$ and Q^* is to be obtained from quadratic equation as follows:

$$a_0 {Q^*}^2 + a_1 Q^* + a_2 = 0, \tag{3.3}$$

where,

$$\begin{aligned} a_0 &= \nu f(1-\delta), \\ a_1 &= \eta b f(1-\delta)(P^*)^2 + bfP^* + \eta z_1 f(1-\delta)^2 P^* + \nu(1-\delta) + z_1(1-\delta)f, \\ a_2 &= \eta b(1-\delta)(P^*)^2 + bP^* - \eta r_1(1-\delta)P^* - r_1 + z_1(1-\delta) + \eta z_1(1-\delta)^2. \end{aligned}$$

We can see that $a_0 > 0$ and $a_1 > 0$. Using quadratic equation root properties, equation (2.3) has a positive root if $a_2 < 0$, that is

$$r_1(1+\eta(1-\delta)P^*) > bP^*(1+\eta(1-\delta)P^*) + z_1(1-\delta)(1+\eta(1-\delta)),$$

with $Q^* = \frac{-a_1+\sqrt{a_1^2-4a_0a_2}}{2a_0}$. Furthermore, the interior equilibrium point $E_2 = (P^*, Q^*)$ exists under condition $c\nu > \eta(r_2+z_2)$ and $r_1(1+\eta(1-\delta)P^*) > bP^*(1+\eta(1-\delta)P^*) + z_1(1-\delta)(1+\eta(1-\delta))$.

The Jacobian matrix of model (2.10) at any eqilibrium point (P,Q) is given by

$$J(P,Q) = \begin{bmatrix} K_{11} & K_{12} \\ K_{21} & K_{22} \end{bmatrix},$$

where,

$$K_{11} = 1 + \frac{h^\alpha}{\Gamma(1+\alpha)}\left[\frac{r_1}{1+fQ} - 2bP - \frac{\nu(1-\delta)Q}{1+\eta(1-\delta)P} + \frac{\eta\nu(1-\delta)^2PQ}{(1+\eta(1-\delta)P)^2} - z_1(1-\delta)\right],$$
$$K_{12} = -\frac{h^\alpha}{\Gamma(1+\alpha)}\left[\frac{r_1fP}{(1+fQ)^2} + \frac{\nu(1-\delta)P}{1+\eta(1-\delta)P}\right],$$
$$K_{21} = \frac{h^\alpha}{\Gamma(1+\alpha)}\left[\frac{c\nu(1-\delta)Q}{(1+\eta(1-\delta)P)^2}\right],$$
$$K_{22} = 1 + \frac{h^\alpha}{\Gamma(1+\alpha)}\left[-r_2 + \frac{c\nu(1-\delta)P}{1+\eta(1-\delta)P} - z_2\right].$$

Theorem 3.1. *Let* $h_1 = \left[\frac{2\Gamma(1+\alpha)}{z_1(1-\delta)-r_1}\right]^{\frac{1}{\alpha}}$, $h_2 = \left[\frac{2\Gamma(1+\alpha)}{r_2+z_2}\right]^{\frac{1}{\alpha}}$ *and* $z_1(1-\delta) > r_1$. *Therefore the trivial equilibrium point* $E_0 = (0,0)$ *is*

1. *sink if* $h < \min\{h_1, h_2\}$;
2. *source if* $h > \max\{h_1, h_2\}$;
3. *saddle if* $h_1 < h < h_2$ *or* $h_2 < h < h_1$;
4. *non-hyperbolic if* $h = h_1$ *or* $h = h_2$.

Proof. The Jacobian matrix at the equilibrium point $E_0 = (0,0)$ is,

$$J(E_0) = \begin{bmatrix} 1 + \frac{h^\alpha}{\Gamma(1+\alpha)}(r_1 - z_1(1-\delta)) & 0 \\ 0 & 1 - \frac{h^\alpha}{\Gamma(1+\alpha)}(r_2+z_2) \end{bmatrix},$$

which gives $\lambda_1 = 1 + \frac{h^\alpha}{\Gamma(1+\alpha)}(r_1 - z_1(1-\delta))$ and $\lambda_2 = 1 - \frac{h^\alpha}{\Gamma(1+\alpha)}(r_2+z_2)$. Since $z_1(1-\delta) > r_1$, then we get $h_1 > 0$. We can easily prove that if $h < h_1$ then $|\lambda_1| < 1$; if $h > h_1$ then $|\lambda_1| > 1$; if $h = h_1$ then $|\lambda_1| = 1$. Also if $h < h_2$ then $|\lambda_2| < 1$; if $h > h_2$ then $|\lambda_2| > 1$; if $h = h_2$ then $|\lambda_2| = 1$. □

Theorem 3.2. *Let* $h_3 = \left[\frac{2\Gamma(1+\alpha)}{r_1-z_1(1-\delta)}\right]^{\frac{1}{\alpha}}$, $h_4 = \left[\frac{2\Gamma(1+\alpha)}{(r_2+z_2)-\frac{c\nu(1-\delta)(r_1-z_1(1-\delta))}{b+\eta(1-\delta)(r_1-z_1(1-\delta))}}\right]^{\frac{1}{\alpha}}$ *and* $r_2+z_2 > \frac{c\nu(1-\delta)(r_1-z_1(1-\delta))}{b+\eta(1-\delta)(r_1-z_1(1-\delta))}$. *Therefore the trivial equilibrium point* $E_1 = (\frac{r_1-z_1(1-\delta)}{b}, 0)$ *is*

1. *sink if* $h < \min\{h_3, h_4\}$*;*
2. *source if* $h > \max\{h_3, h_4\}$*;*
3. *saddle if* $h_3 < h < h_4$ *or* $h_4 < h < h_3$*;*
4. *non-hyperbolic if* $h = h_3$ *or* $h = h_4$*.*

Proof. The Jacobian matrix at equilibrium point $E_1 = (\frac{r_1 - z_1(1-\delta)}{b}, 0)$ is,

$$J(E_1) = \begin{bmatrix} L_{11} & L_{12} \\ 0 & L_{22} \end{bmatrix},$$

where,

$$\begin{aligned}
L_{11} &= 1 + \frac{h^\alpha}{\Gamma(1+\alpha)} \left[-r_1 + z_1(1-\delta)\right], \\
L_{12} &= -\frac{h^\alpha}{\Gamma(1+\alpha)} \left[\frac{r_1 f(r_1 - z_1(1-\delta))}{b} + \frac{\nu(1-\delta)(r_1 - z_1(1-\delta))}{b + \eta(1-\delta)(r_1 - z_1(1-\delta))}\right], \\
L_{22} &= 1 + \frac{h^\alpha}{\Gamma(1+\alpha)} \left[-(r_2 + z_2) + \frac{c\nu(1-\delta)(r_1 - z_1(1-\delta))}{b + \eta(1-\delta)(r_1 - z_1(1-\delta))}\right],
\end{aligned}$$

which gives

$$\lambda_1 = 1 + \frac{h^\alpha}{\Gamma(1+\alpha)} \left[-r_1 + z_1(1-\delta)\right]$$

and

$$\lambda_2 = 1 + \frac{h^\alpha}{\Gamma(1+\alpha)} \left[-(r_2 + z_2) + \frac{c\nu(1-\delta)(r_1 - z_1(1-\delta))}{b + \eta(1-\delta)(r_1 - z_1(1-\delta))}\right].$$

Since $r_2 + z_2 > \frac{c\nu(1-\delta)(r_1 - z_1(1-\delta)}{b+\eta(1-\delta)(r_1 - z_1(1-\delta))}$, then we get $h_4 > 0$. We can easily prove that if $h < h_3$ then $|\lambda_1| < 1$; if $h > h_3$ then $|\lambda_1| > 1$; if $h = h_3$ then $|\lambda_1| = 1$. Also if $h < h_4$ then $|\lambda_2| < 1$; if $h > h_4$ then $|\lambda_2| > 1$; if $h = h_4$ then $|\lambda_2| = 1$. □

Theorem 3.3. *Suppose that*

$$\begin{aligned}
\Delta = &\left[-bP^* + \frac{\eta\nu(1-\delta)^2 P^* Q^*}{\left(1 + \eta(1-\delta)P^*\right)^2}\right]^2 \\
&- 4\left[\frac{\left(r_1 f c Q^* + (1 + fQ^*)^2(r_2 + z_2)\right)\nu(1-\delta)Q^*}{(1 + fQ^*)^2\left(1 + \eta(1-\delta)P^*\right)^2}\right],
\end{aligned}$$

and

$$h_5 = \left[\Gamma(1+\alpha)\left(\frac{-J_{11} + \sqrt{J_{11}^2 - 4J_{12}J_{21}}}{J_{12}J_{21}}\right)\right]^{1/\alpha},$$

$$h_6 = \left[\Gamma(1+\alpha)\left(\frac{-J_{11} - \sqrt{J_{11}^2 - 4J_{12}J_{21}}}{J_{12}J_{21}}\right)\right]^{1/\alpha},$$

$$h_7 = \left[\frac{-\Gamma(1+\alpha)\, J_{11}}{J_{12}J_{21}}\right]^{1/\alpha}.$$

Therefore, the trivial equilibrium point $E_2 = (P^*, Q^*)$ *is a*

1. *sink if one of the following conditions are satisfied:*
   - $\Delta < 0$ *and* $h < h_7$,
   - $\Delta \geq 0$ *and* $h < h_6$,
2. *source if any of the following conditions are accomplished:*
   - $\Delta < 0$ *and* $h > h_7$,
   - $\Delta \geq 0$ *and* $h > h_5$,
3. *saddle if* $\Delta \geq 0$ *and* $h_6 < h < h_5$,
4. *non-hyperbolic if any of the following conditions are accomplished:*
   - $\Delta < 0$ *and* $h = h_7$,
   - $\Delta > 0$ *and* $h = h_5$ *or* $h = h_6$.

Proof. The Jacobian matrix at $E_2 = (P^*, Q^*)$ is

$$J(E_2) = \begin{bmatrix} 1 + \frac{h^\alpha}{\Gamma(1+\alpha)} J_{11} & -\frac{h^\alpha}{\Gamma(1+\alpha)} J_{12} \\ \frac{h^\alpha}{\Gamma(1+\alpha)} J_{21} & 1 \end{bmatrix}$$

where,

$$J_{11} = -bP^* + \frac{\eta\nu(1-\delta)^2 P^* Q^*}{(1+\eta(1-\delta)P^*)^2},$$
$$J_{12} = \frac{r_1 f P^*}{(1+fQ^*)^2} + \frac{r_2 + z_2}{c},$$
$$J_{21} = \frac{c\nu(1-\delta)Q^*}{(1+\eta(1-\delta)P^*)^2}.$$

The characteristic equation of $J(E_2)$ is $\lambda^2 - Tr(J(E_2))\lambda + Det(J(E_2)) = 0$, with $Tr(J(E_2)) = 2 + \frac{h^\alpha}{\Gamma(1+\alpha)} \left[-bP^* + \frac{\eta\nu(1-\delta)^2 P^* Q^*}{(1+\eta(1-\delta)P^*)^2}\right]$ and

$$\begin{aligned} Det(J(E_2)) = & \left[1 + \frac{h^\alpha}{\Gamma(1+\alpha)} \left(-bP^* + \frac{\eta\nu(1-\delta)^2 P^* Q^*}{(1+\eta(1-\delta)P^*)^2}\right)\right] \\ & + \left[\frac{h^\alpha}{\Gamma(1+\alpha)}\right]^2 \left[\frac{\left(r_1 f c Q^* + (1+fQ^*)^2 (r_2 + z_2)\right)\nu(1-\delta)Q^*}{(1+fQ^*)^2\,(1+\eta(1-\delta)P^*)^2}\right]. \end{aligned}$$

□

From a biological perspective, the stability of each equilibrium point represents different ecological outcomes. The trivial equilibrium point $E_0 = (0, 0)$ indicates extinction of both prey and predator populations. Its stability implies that under certain conditions such as excessive harvesting or lack of prey refuge, the ecosystem may collapse. The predator-free equilibrium point E_1 reflects scenarios where prey survive but predators die out, which may occur if predation pressure is insufficient to sustain the predator population or if prey have strong protection. In contrast, the interior equilibrium point $E_2 = (P^*, Q^*)$ corresponds to the coexistence of both species in a balanced ecosystem. Stability at this point biologically implies a resilient system where fear effects, refuge, and harvesting interact to create a self-regulating environment. Thus, the mathematical conditions for local stability or bifurcation directly translate to biological insights on population persistence, extinction risks, and ecological balance.

4. Numerical simulation

In this section, we conduct numerical simulations for the discrete system with fractional order. In this numerical simulation, we perform some scenarios. The following scenarios have been used to categorize various numerical outcomes of model simulation and their corresponding observations:

Example 4.1. Examination of the model system dynamics in the absence of the fear effect. Let $r_1 = 2, \nu = 0.5, c = 0.8, \eta = 0.1, z_1 = 0.2, z_2 = 0.1, r_2 = 0.4$ and $b = 0.1$. We performed an analysis of the dynamics of the model system (2.10) by varying the model parameters δ, assuming the absence of the fear effect $f = 0$ in the system. We have investigated the impact of refuge in the absence of fear effect. In this case we use some parameters $\delta = 0.2$ and $\delta = 0.8$. Assuming a fixed value of $\alpha = 0.9$, we incrementally raise the parameter of the prey refuge δ within the range of $[0, 1)$. The dynamical behavior of the solution of the model system (2.10) near the interior equilibrium point is seen to transition from its unstable periodic limit cycle oscillations to a stable regime. This transition of dynamics has been demonstrated in Figure 1. Figures 1 (a) and (b) respectively represent the time series and phase portrait when $\delta = 0.2$, Figures 1(c) and (d) illustrate the time series and phase portrait, respectively, when $\delta = 0.8$. These figures clearly demonstrate a stable steady state. It should be emphasized that a consistent increase in the rate of prey refuge guarantees a corresponding increase in the biomass of the prey population.

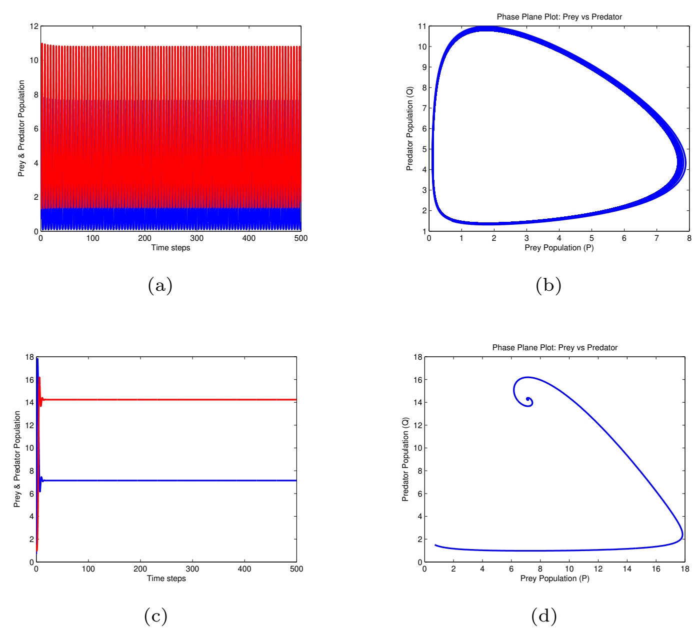

Figure 1. Dynamical behavior of the model system for different values of prey refuge δ, and fear effect $f = 0$ in the system. The graphs (a) and (b) represent the time series and phase portrait of the solutions of the model when $\delta = 0.2$; the graphs (c) and (d) represent the time series and phase portrait of the solutions of the model when $\delta = 0.8$.

In the context of biology, the simulation in Example 4.1 demonstrates the significant role of prey refuge in maintaining ecosystem stability. The prey refuge parameter (δ) can be associated with real-world protective measures, such as the presence of hiding spots (e.g., bushes or caves) that reduce direct interactions between predators and prey. In this simulation, when the level of prey refuge increases, the prey population tends to reach a more stable steady state, ultimately reducing excessive fluctuations in both predator and prey populations.

From an ecological perspective, this highlights the importance of preserving natural habitats that provide refuge for prey, ensuring population stability. When prey have adequate protection, the risk of drastic population decline due to predation decreases, preventing imbalances within the ecosystem and sustaining the food chain. Therefore, habitat conservation is a crucial element in ecosystem management to mitigate negative impacts on both prey and predator species.

Example 4.2. The dynamics of the model system in the absence of a prey refuge. Taking $r_1 = 2, \nu = 0.5, c = 0.8, \eta = 0.1, z_1 = 0.2, z_2 = 0.1, r_2 = 0.4$ and $b = 0.1$. In this example, we have presupposed that the system lacks a prey refuge and have investigated the dynamics of the model system (2.10) by adjusting the model parameter fear f. In this study, we have set the value of $\alpha = 0.9$ constant and incrementally raised the parameter of the fear effect f within the range of 0 to 5. The dynamical behavior of the solution of the model system (2.10) near the interior equilibrium point $E_2 = (2.6316, 5.6566)$ is seen to transition from its initially unstable periodic limit cycle oscillations to a stable state. This transition of dynamics has been demonstrated in Figure 2. The time series and phase portrait for $f = 0.1$ are shown in Figures 2 (a) and (b), respectively. Similarly, Figures 2(c) and (d) depict the time series and phase portrait for $f = 2$, respectively. These figures clearly demonstrate the stable steady state of the interior equilibrium point $E_2 = (1.429, 2.801)$. It should be emphasized that when there is no prey refuge, our proposed model system displays unstable system dynamics when the fear effect is at a low level.

From a biological perspective, the fear effect represents behavioral changes in prey due to the presence of predators, such as reducing movement, foraging less, or seeking cover. This behavior can decrease encounters with predators, indirectly reducing predation rates. The simulation shows that, in the absence of physical refuge, the psychological impact of fear alone can lead to population stability by limiting risky behaviors that would increase vulnerability.

This reflects a fundamental ecological concept known as the “landscape of fear,” where the presence of predators changes the spatial and behavioral patterns of prey, ultimately affecting overall population dynamics. The model emphasizes the importance of predator-prey interactions not only through direct predation but also through the influence of fear, which can help maintain ecological balance even in the absence of physical refuges.

Example 4.3. The dynamics of the model system in the absence of harvesting in both population. Consider the parameter value $r_1 = 2, \nu = 0.5, c = 0.8, \eta = 0.1, \delta = 0.1, r_2 = 0.4$ and $b = 0.1$. In this example, we investigated the impact of fear in absence of harvesting $(z_1, z_2 = 0)$. The value of $\alpha = 0.9$ has been held constant, while the parameter of fear effect f is incrementally increased within the interval $(0, 5)$. The dynamical behavior of the solution of the model system (2.10) near the interior equilibrium point $E_2 = (1.235, 3.385)$ is seen to transition from its unstable periodic limit cycle oscillations to a stable state. This transition of dynamics has been demonstrated in Figure 3. Figures 3(a) and (b) depict the time series and phase

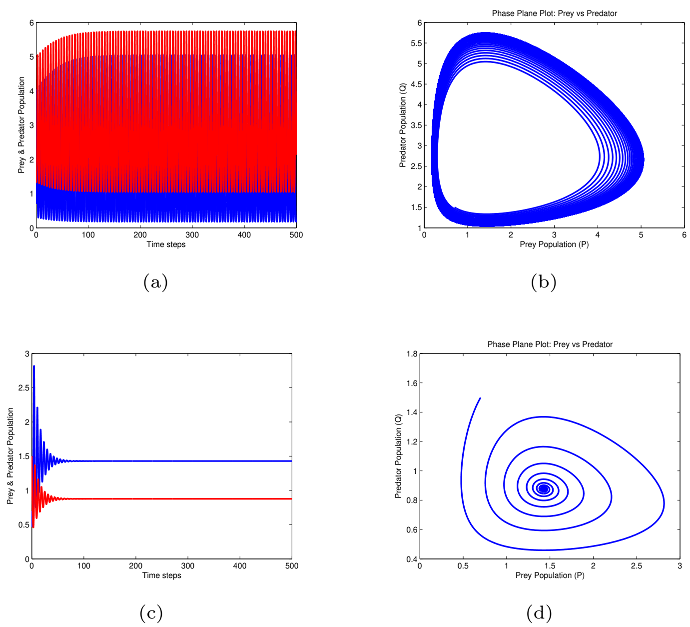

Figure 2. Dynamical behavior of the model system for varying values of fear f and prey refuge $\delta = 0$ in the system. The time series and phase portrait of the model's solutions when $f = 0.1$ are depicted in the graphs (a) and (b), while the time series and phase portrait of the model's solutions when $f = 2$ are depicted in the graphs (c) and (d).

portrait, respectively, when $f = 0.1$. Figures 3(c) and (d) present the time series and phase portrait, respectively, when $f = 2$. These figures clearly demonstrate the stable steady state of the interior equilibrium point $E_2 = (1.235, 3.385)$.

Biologically, this example emphasizes the significant role of fear as a natural regulatory mechanism in ecosystems where human intervention, such as harvesting or culling, is not present. The absence of harvesting implies that no external pressures are reducing population numbers, so internal factors, such as fear, become crucial in stabilizing population dynamics. Fear can reduce predator-prey encounters, allowing prey populations to avoid excessive predation and maintain a balanced growth rate, thus contributing to stability within the ecosystem.

This finding suggests that fear-driven behavioral changes can serve as a natural stabilizer in ecosystems without human exploitation. The absence of harvesting means that the prey population is left to manage its interactions with predators solely through behavior, such as avoiding high-risk areas. Such natural mechanisms underscore the importance of maintaining intact predator-prey relationships to ensure ecological stability and balance without overreliance on human management interventions like culling or artificial regulation.

Example 4.4. Taking the parameter values $\alpha = 0.9, r_1 = 0.1, f = 2, \nu = 0.3, c = 0.1, \eta = 0.5, z_1 = 1, z_2 = 0.9, r_2 = 0.8$ and $b = 0.5$, we show the stability of the trivial equilibrium point $E_0 = (0, 0)$. In this case, we use parameter $\alpha = 0.9, h = 0.1$, and initial point $P_0 = 0.7,\ Q_0 - 1.5$. According to Theorem 3.1, $E_0 = (0, 0)$ is sink (stable) if $h < \min\{h_1, h_2\}$, with $h_1 = 26.7163, h_2 = 1.1471$. The time series and phase portrait of the system (2.10) are shown in Figure 4.

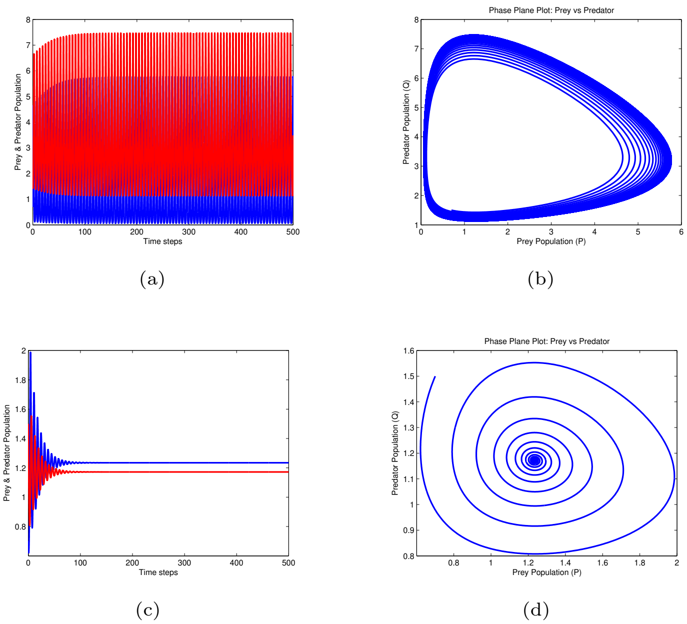

Figure 3. Dynamical behavior of the model system for varying values of fear f and harvesting $z_1 = z_2 = 0$ in the system. The graphs (a) and (b) illustrate the time series and phase portrait of the model's solutions at $f = 0.1$, while the graphs (c) and (d) illustrate the time series and phase portrait of the model's solutions at $f = 2$.

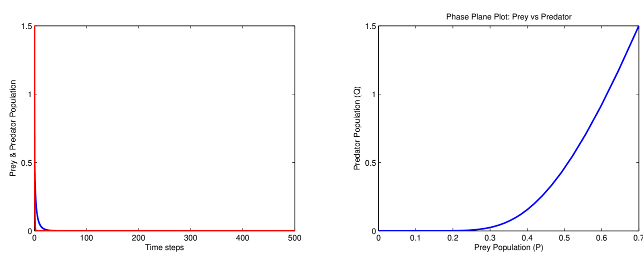

Figure 4. Time series and phase portrait are stable at equilibrium point $E_0(0, 0)$

Example 4.5. Let the parameter values $r_1 = 0.8, f = 2, \nu = 0.3, c = 0.1, \eta = 0.5, z_1 = 1, z_2 = 0.9, r_2 = 0.8, \delta = 0.8$ and $b = 0.5$. We show the stability of the trivial equilibrium point $E_1 = (1.2, 0)$. In this case, we use parameter $\alpha = 0.9, h = 0.1$. According to Theorem 3.2, $E_1 = (1.2, 0)$ is sink (stable) if $h < \min\{h_3, h_4\}$, with $h_1 = 3.6489, h_2 = 1.152$. The plot of P_n and Q_n are shown in Figure 5. In this simulation, we also show the bifurcation diagram in interval $5 < h < 7.5$ when $\alpha = 0.9$ and in interval $11 < h < 13$ when $\alpha = 0.7$. See Figure 6.

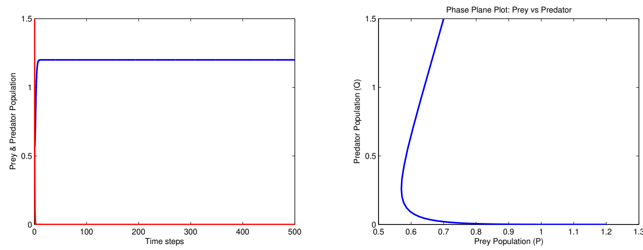

Figure 5. Time series and phase portrait are stable at equilibrium point $E_1(1.2, 0)$

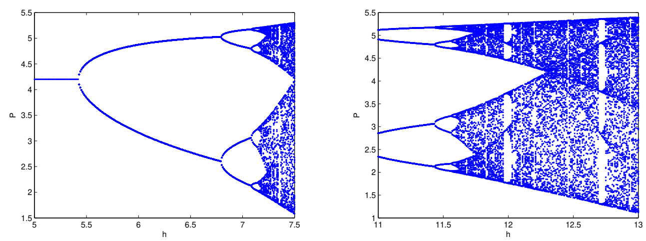

Figure 6. Bifurcation diagram of the system (2.2) in interval $5 < h < 7.5, \alpha = 0.9$ and in interval $11 < h < 13, \alpha = 0.7$.

Example 4.6. Choosing the parameter values $\alpha = 0.9, r_1 = 0.5, f = 5, \nu = 3, c = 0.8, \delta = 0.8, \eta = 0.1, z_1 = 0.2, z_2 = 0.0001, r_2 = 0.4$ and $b = 0.1$, we show the stability of co-existence equilibrium point. We use parameter $h = 0.01$, $\alpha = 0.9$ and initial point $P_0 = 0.7,\ Q_0 = 1.5$. In this case, we get co-existence equilibrium point $E_2 = (0.8477, 0.2059)$, $\Delta = -0.0848 < 0\ h_7 = 0.8028$. According to Theorem 3.3, E_2 is sink if $\Delta < 0$ and $h < h_7$. The plot of this simulation in Figure 7. We also perform the bifurcation diagram in interval $0.5 < h < 1.5$ that given in Figure 8.

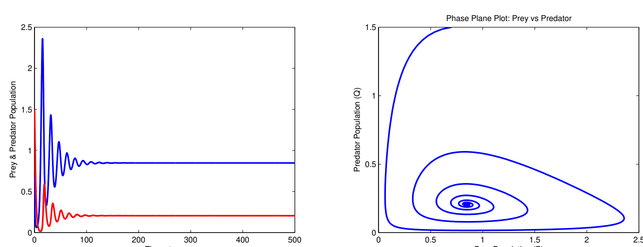

Figure 7. Time series and phase portrait are stable at equilibrium point $E_2(0.8477, 0.2059)$

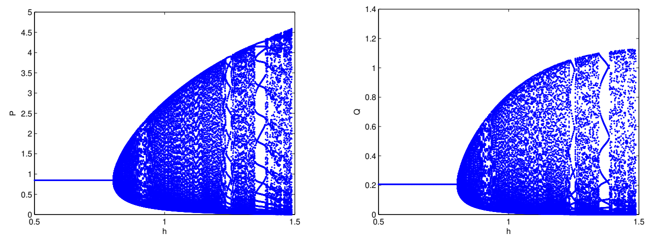

Figure 8. Bifurcation diagram of the system (2.10) in interval $0.5 < h < 1.5$

Sensitivity analysis

To assess the robustness of the model under variations in parameter values, we conducted a sensitivity analysis using Partial Rank Correlation Coefficients (PRCC). The results, illustrated in Figure 9, highlight the influence of each parameter on three key outcomes: prey population, predator population, and system stability.

For the prey population, the parameters with the highest positive impact are the prey intrinsic growth rate (r_1) and the fear level (f), suggesting that increases in these parameters significantly enhance prey biomass. Conversely, the harvesting rate (z_1) and the interaction coefficient (η) show strong negative influence, indicating that elevated harvesting or stronger predator-prey interaction reduces prey numbers.

Regarding the predator population, the most influential parameter is the predation rate (ν), with a strong positive PRCC, implying that higher predation efficiency supports predator growth. In contrast, predator harvesting rate (z_2) and the refuge effect (δ) exhibit a strong negative influence, demonstrating their roles in limiting predator success.

For system stability, while most parameters exhibit relatively small PRCC values, it is observed that higher values of the refuge parameter (δ), harvesting parameters (z_1, z_2), and predation rate (ν) contribute positively to system stability. On the other hand, interaction-related parameters such as (η) have a mild negative effect, likely due to their influence on dynamic feedback loops within the system.

These results underline the importance of carefully managing ecological factors such as fear, refuge, and harvesting in predator-prey dynamics. Parameters associated with external control (like f, z_1, z_2) appear to be key levers for regulating both population levels and ecological stability.

5. Conclusion

This study explores the dynamics of a discrete fractional-order predator-prey model, emphasizing the impact of fear, refuge, and harvesting on prey behavior. Our findings show that fear significantly stabilizes the system by reducing predator-prey interactions, while refuge and harvesting lead to more complex, oscillatory dynamics. These results highlight the significance of fractional-order models in capturing memory-dependent biological processes, providing a more accurate representation of real-world ecological systems.

Despite its strengths, the study has several limitations. The model assumes homogeneous conditions, fixed harvesting rates, and focuses on a single predator-prey

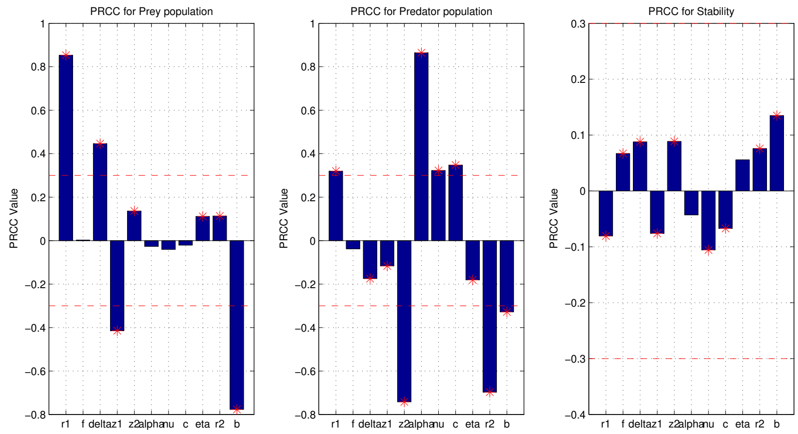

Figure 9. PRCC sensitivity analysis results for prey population (left), predator population (middle), and system stability (right).

pair. These simplifications may limit the generalizability of the findings. Potential risks include over-reliance on specific parameter ranges that may not accurately reflect more dynamic ecosystems, which could lead to misinterpretations when applied to real-world scenarios.

To address these issues, future research could explore spatial heterogeneity, variable harvesting strategies, and multi-species interactions. Incorporating stochastic elements or environmental fluctuations could also provide a more comprehensive understanding of ecosystem dynamics. Additionally, extending the model to continuous-time frameworks or exploring different fractional-order derivatives may offer deeper insights.

The potential applications of this model are vast, particularly in the fields of wildlife management and conservation. By understanding how fear, refuge, and harvesting influence population dynamics, policymakers can develop more sustainable strategies for managing predator-prey systems in the face of human intervention and environmental changes.

Acknowledgements

This work was funded by Indonesian Education Scholarship [ID: 202209090769], Center for Higher Education Funding and Assessment, and Indonesian Endowment Fund for Education.

References

[1] R. Charles, O.D. Makinde and M. Kung'aro, *A review of the mathematical models for the impact of seasonal weather variation and infections on prey predator interactions in serengeti ecosystem*, Open Journal of Ecology, 2022, 12(11), 718–732.

[2] S. Pal, N. Pal, S. Samanta and J Chattopadhyay, *Effect of hunting cooperation and fear in a predator-prey model*, Ecological Complexity, 2019, 39, 100770–100802.

[3] K. Antwi-Fordjour, R.D. Parshad and M.A. Beauregard, *Dynamics of a predator-prey model with generalized Holling type functional response and mutual interference*, Mathematical biosciences, 2020, 326, 108407–108421.

[4] K.B. Blyuss, Y.N. Kyrychko and O.B. Blyuss, *Complex dynamics near extinction in a predator-prey model with ratio dependence and Holling type III functional response*, Frontiers in Applied Mathematics and Statistics, 2022, 8, 1083815–1083822.

[5] H. Zhang, X. Yuan, H. Zou, L. Zhao, Z. Wang, F. Guo and Z. Liu, *The Spatiotemporal Dynamics of Insect Predator-Prey System Incorporating Refuge Effect*, Entropy, 2024, 26(3), 196.

[6] D. Chaturvedi and O.P. Misra, *Impact of habitat destruction and its subsequent regeneration on the dynamics of a Holling type II prey-predator interacting species system with prey refuge*, International Journal of Dynamics and Control, 2024, 12(5), 1332–1345.

[7] O. Francis, T. Aminer, B. Okelo and J. Manyala, *Dynamical Analysis of Prey Refuge Effects on the Stability of Holling Type III Four-species Predator-Prey System*, Results in Control and Optimization, 2024, 14, 100390.

[8] Y. Ma and R. Yang, *Hopf-Hopf bifurcation in a predator-prey model with nonlocal competition and refuge in prey*, Results in Control and Optimization, 2024, 29(6), 2582–2609.

[9] I.M. Kafi, S. Naji and D.M. Alrahal, *Dynamic behavior of predator-prey system with refuge for both species*, AIP Conference Proceedings, 2024, 3097(1). https://doi.org/10.1063/5.0213302.

[10] S. Pal, S. Karmakar, S. Pal, N. Pal, A.K. Misra and J. Chattopadhyay, *Impact of fear and group defense on the dynamics of a predator-prey system*, International Journal of Bifurcation and Chaos, 2024, 34(02), 2450019.

[11] Y. Xue, *Impact of both-density-dependent fear effect in a Leslie-Gower predator-prey model with Beddington-DeAngelis functional response*, Chaos, Solitons & Fractals, 2024, 185, 115055.

[12] M.X. Chen, X.Z. Li and R.C. Wu, *Bifurcations and steady states of a predator-prey model with strong Allee and fear effects*, Int. J. Biomath, 2023. https://doi.org/10.1142/S1793524523500663.

[13] S.N. Afiyah, F. Fatmawati, and W.Windarto, *Dynamical analysis of a leslie-gower predator-prey model with holling type IV functional response incorporating fear and allee effect*, AIP Conference Proceedings, 2025,3302(1), 030001.

[14] R.K. Naji, *Modeling and Analysis of A Prey-Predator System Incorporating Fear, Predator-Dependent Refuge, with Cannibalism In Prey*, Iraqi Journal of Science, 2024, 297–319. https://doi.org/10.24996/ijs.2024.65.1.25.

[15] M. Rayungsari, A. Suryanto, W.M. Kusumawinahyu and I. Darti, *Dynamical analysis of a predator-prey model incorporating predator cannibalism and refuge*, Axioms, 2022,11(3), 116.

[16] D. Duan, B. Niu, J. Wei and Y. Yuan, *The dynamical analysis of a nonlocal predator-prey model with cannibalism*, European Journal of Applied Mathematics, 2024, 1–25.
https://doi.org/10.1017/S0956792524000019.

[17] X. LI, Q.I.N. YUE and F. Chen, *Global Stability of the Positive Equilibrium of a Leslie-Gower Predator-Prey Model Incorporating Predator Cannibalism*, WSEAS Transactions on Systems, 2022, 21, 400–408.

[18] K. Sarkar and B. Mondal, *Bifurcation and dynamic analysis of prey-predator model with combined nonlinear harvesting*, International Journal of Biomathematics, 2024, 2450010.
https://doi.org/10.1142/S1793524524500104.

[19] Y. Zhang and J. Luo, *Bifurcation analysis of a Leslie-type predator-prey system with prey harvesting and group defense*, Frontiers in Physics, 2024, 12, 1392446 2450010.

[20] L. Yu, B.T. Mulugeta, J. Ren and Q. Yuan, *Bifurcation analysis of predator-prey model with Cosner type functional response and combined harvesting*, Authorea Preprints, 2024.
https://doi.org/10.1002/mma.9865.

[21] B. Daşbaşı, *Stability Analysis of Mathematical Model including Pathogen-Specific Immune System Response with Fractional-Order Differential Equations*, Computational and mathematical methods in medicine, 2018, 2018(1), 7930603–7930612.

[22] C. Ionescu, A. Lopes, D. Copot, J.A.T. Machado and J.H.T Bates, *The role of fractional calculus in modeling biological phenomena: A review*, Communications in Nonlinear Science and Numerical Simulation, 2017, 51, 141–159.

[23] M. Das and G.P. Samanta, *A prey-predator fractional order model with fear effect and group defense*, International Journal of Dynamics and Control, 2021, 9, 334–349.

[24] D. Mukherjee, *Dynamical study of non-integer order predator-prey system with fear effect*, International Journal of Modelling and Simulation, 2022, 42(3), 441–449.

[25] E. Rahmi, I. Darti, A. Suryanto and T. Trisilowati, *A modified Leslie-Gower model incorporating Beddington-DeAngelis functional response, double Allee effect and memory effect*, Fractal and Fractional, 2021, 5(3), 84.

[26] A. Suryanto, I. Darti and S. Anam, *Stability Analysis of a Fractional Order Modified Leslie-Gower Model with Additive Allee Effect*, International Journal of Mathematics and Mathematical Sciences, 2017, 2017(1), 8273430.

[27] F.B. Yousef, A. Yousef and C. Maji, *Effects of fear in a fractional-order predator-prey system with predator density-dependent prey mortality*, Chaos, Solitons & Fractals, 2021, 145, 110711.

[28] S.N. Afiyah, F. Fatmawati, W. Windarto, and A. Abidemi, *Dynamics of a Fractional Order Harvested Predator-Prey Model Incorporating Fear Effect and Refuge*, Statistics, Optimization & Information Computing, 2025, 13(4), 1690–1713.

[29] H. Zhang, Y. Cai, S. Fu, W. Wang, *Impact of the fear effect in a prey-predator model incorporating a prey refuge*, Applied Mathematics and Computation, 2019, 356, 328–337.

[30] K. Sarkar, B. Mondal, *Dynamic analysis of a fractional-order predator-prey model with harvesting*, Int. Journal of Dynamics and Control, 2023, 11, 1518–1531.

[31] P. Das, D. Mukherjee and A.K. Sarkar, *Study of an SI epidemic model with nonlinear incidence rate: discrete and stochastic version*, Applied Mathematics and Computation, 2011, 218(6), 2509–2515.

[32] K. Diethelm, *The analysis of fractional differential equations, volume 2004 of Lecture Notes in Mathematics*, Springer-Verlag, Berlin, 2010.

[33] A.A. Elsadany and A.E. Matouk, *Dynamical behaviors of fractional-order Lotka-Volterra predator-prey model and its discretization*, Journal of Applied Mathematics and Computing, 2015, 49, 269–283.

[34] H.S. Panigoro, E. Rahmi, N. Achmad, S.L. Mahmud, R. Resmawan and A.R. Nuha, *A discrete-time fractional-order Rosenzweig-Macarthur predator-prey model involving prey refuge*, Commun. Math. Biol. Neurosci., 2021, 2021(77), 1–9.

[35] R.P. Agarwal, A.M.A. El-Sayed and S.M. Salman, *Fractional-order Chua's system: discretization, bifurcation and chaos*, Advances in Difference Equations, 2013, 2013, 1–13.

[36] A. Aldurayhim, A.A. Elsadany and A. Elsonbaty, *On dynamic behavior of a discrete fractional-order nonlinear prey-predator model*, Fractals, 2021, 29(08), 2140037.

[37] D. Aruğaslan and A.Ö. zer, *Stability analysis of a predator-prey model with piecewise constant argument of generalized type using Lyapunov functions*, Journal of Mathematical Sciences, 2014, 203, 297–305.

[38] Q. Din, *Complexity and chaos control in a discrete-time prey-predator model*, Communications in nonlinear science and numerical simulation, 2017, 49, 113–134.

[39] A.M.A. El-Sayed and S.M. Salman, *On a discretization process of fractional-order Riccati differential equation*, J. Fract. Calc. Appl, 2013, 4(2), 251–259.

[40] M.J. Uddin, S.M.S. Rana, S. Işık and F. Kangalgil, *On the qualitative study of a discrete fractional order prey-predator model with the effects of harvesting on predator population*, Chaos, Solitons & Fractals, 2023, 175, 113932.